1-1-2012

Experimental and computational simulation of beta-dose heterogeneity in sediment

Alastair C. Cunningham
Delft University of Technology, acunning@uow.edu.au

Daniel J. De Vries
Delft University of Technology

Dennis R. Schaart
Delft University of Technology

Experimental and computational simulation of beta-dose heterogeneity in sediment

Abstract

Interpreting the spread in equivalent-dose estimates is an important aspect of optically stimulated luminescence (OSL) dating. Ideally, prior to age estimation, an assessment should be made of the likely spread in equivalent dose due to dose-rate heterogeneity in the sediment. Such a procedure would greatly increase the validity of OSL ages, particularly for sediments susceptible to partial bleaching, and for sediments with coarse or poorly sorted grain-size distributions. In this paper we take a step towards a general model of dose-rate heterogeneity by simulating the 40K-derived beta dose to quartz. We present an experimental simulation of the 40K beta dose, and compare the results with a Monte Carlo simulation of the same experiment. The experiment uses artificially produced 24Na to simulate the 40K beta dose to quartz, allowing a large, heterogeneous dose to be administered in a short period of time. The Monte Carlo simulation correctly predicts the shape of the equivalent-dose distribution, but underestimates the spread in dose received by different grains. The experimental set-up provides a new avenue of research into beta-dose heterogeneity.

Keywords

CAS

Disciplines

Medicine and Health Sciences | Social and Behavioral Sciences

Publication Details

Cunningham, A. C., De Vries, D. J. & Schaart, D. R. (2012). Experimental and computational simulation of beta-dose heterogeneity in sediment. Radiation Measurements, 47 (11-12), 1060-1067.

Experimental and computational simulation of beta-dose heterogeneity in sediment

Alastair C. Cunningham[1], Daniel J. DeVries[2], Dennis R. Schaart[2]

[1]Netherlands Centre for Luminescence dating, Delft University of Technology, Mekelweg 15, 2629 JB Delft, the Netherlands

[2]Radiation and Isotopes for Health, Delft University of Technology, Mekelweg 15, 2629 JB Delft, the Netherlands

Email: blinkysimpson@hotmail.com

Abstract

Interpreting the spread in equivalent-dose estimates is an important aspect of optically stimulated luminescence (OSL) dating. Ideally, prior to age estimation, an assessment should be made of the likely spread in equivalent dose due to dose-rate heterogeneity in the sediment. Such a procedure would greatly increase the validity of OSL ages, particularly for sediments susceptible to partial bleaching, and for sediments with coarse or poorly sorted grain-size distributions. In this paper we take a step towards a general model of dose-rate heterogeneity by simulating the ^{40}K-derived beta dose to quartz. We present an experimental simulation of the ^{40}K beta dose, and compare the results with a Monte Carlo simulation of the same experiment. The experiment uses artificially produced ^{24}Na to simulate the ^{40}K beta dose to quartz, allowing a large, heterogeneous dose to be administered in a short period of time. The Monte Carlo simulation correctly predicts the shape of the equivalent-dose distribution, but underestimates the spread in dose received by different grains. The experimental set-up provides a new avenue of research into beta-dose heterogeneity.

Keywords: OSL, luminescence, dating, heterogeneity, Monte Carlo, beta-dose, overdispersion, scatter, single grain, partial bleaching

1. Introduction

Mineral grains from natural sediment are increasingly used to determine the age of sediment deposition. The optically stimulated luminescence (OSL) signal is used to determine the radiation dose received by the mineral grains since the last burial episode. When combined with an estimate of the dose rate to the grains in the natural setting, the age of the sediment can be determined. Wintle (2008), and Rhodes (2011) provide an overview of the method.

Quartz is the mineral most commonly used for dating. For any single sample, OSL measurements are made on a number of subsamples (aliquots), which may contain a single grain or multiple grains of quartz. The equivalent dose (D_e) is determined for each aliquot, providing a distribution of D_e values from which the burial dose is estimated. The D_e values are rarely consistent with a common burial dose; there is usually more scatter in the data than can be expected from Poisson statistics alone.

Understanding the source of scatter in D_e is vital for OSL dating. A misinterpretation of the source of scatter can lead to an inaccurate age estimate, because the estimate of the burial dose is dependent on how the scatter is interpreted. For example, where scatter is attributed to insufficient bleaching, an age model will be chosen that assigns a burial dose consistent with the younger part of the D_e distribution; should the interpretation be wrong, then the burial-dose (and hence the age) is likely to be an underestimate.

For determining the burial dose for partially bleached samples, it is necessary to estimate the amount of variation that could be expected in the data in the absence of partial bleaching. One way to do this is to examine the D_e distributions found with indisputably well-bleached samples, for which a relative standard deviation of 20% is typical at the single grain level (Duller, 2008). However, there is a considerable amount of variation between different samples (e.g. Arnold and Roberts, 2009), which suggests that physical differences between samples, such as grain size or mineralogy, may influence the spread in the data. The mechanism for this effect is known as beta-dose heterogeneity, or microdosimetric variation. It is caused by the non-uniform distribution of beta-emitting radionuclides in the sediment, combined with the short range of beta particles. The consequence is that the beta dose rate may be different for each grain of quartz. As beta radiation typically accounts for around half of the total dose to quartz, heterogeneity in the beta dose is likely to be a significant source of scatter in D_e.

Typically around 90% of the beta dose to quartz comes from the decay of ^{40}K, which occurs at high concentrations in K-feldspars and some clay minerals. Grains of K-feldspar could act as 'hotspots' of activity, leading to positively skewed D_e distributions (Mayya et al., 2006). It is likely that the extent of the effect is dependent on physical parameters of the sediment, particularly the grain-size distribution and concentration of K-feldspar grains. Ideally, an assessment of the likely influence of hotspots would be made for each OSL sample. Such an approach would be based on a general model of dose-rate heterogeneity, something which does not yet exist. A possible source of such a model would be through a series of Monte Carlo simulations of energy deposition, in combination with experimental validation.

Studies of beta-dose heterogeneity have been limited in number. Monte Carlo calculations can be complex, while experiments simulating the natural dose rate may take many months to perform. Nathan et al. (2003) investigated the influence of macrobodies within artificial sediment, and showed the benefit of Monte Carlo techniques when combined with experimental methods. Monte Carlo methods have also proven useful in determining the mean dose rate, regardless of scatter between grains (Grine et al., 2007; Cunningham et al., 2011). Kalchgruber et al. (2003) and Nathan et al. (2003) also performed experimental measurements of dose rate heterogeneity, using grains of Al_2O_3:C to record the dose in natural or artificial sediment over a period of time.

This paper takes a different approach to the analysis of dose-rate variation in sediment. Starting from the assumption that the principle source of scatter is the K-feldspar 'hotspot' hypothesis of Mayya et al. (2006), we design an experiment to determine the likely effect of these hotspots under extreme conditions. Our approach combines experimental and Monte Carlo simulations, and is very efficient in terms of experimental duration. The set-up we describe does not provide a true representation of nature, but could provide a practical framework for investigating dose-rate heterogeneity in sediment.

2. Experimental Simulation

2.1 Approach

We constructed a 'sand box' experiment, in which grains of quartz were mixed with beta-emitting hotspot grains. Rather than using feldspar for the hotspot material, we used spherical grains of sodium hydroxide (NaOH). Before mixing the materials, the NaOH was bombarded with neutrons in a nuclear reactor to produce ^{24}Na. Radioactive ^{24}Na has

a half life of 14.997 ± 12 hours, decaying to ^{24}Mg by the emission of a beta particle and two γ-ray photons. The beta-spectrum of ^{24}Na is almost identical to ^{40}K (Fig. 1), while the gammas are relatively high energy (1.37 MeV and 2.75 MeV). The advantage of this set-up is that a large, heterogeneous beta dose can be given to the quartz grains in a short period of time (~2 weeks), after which the material is safe to handle. The beta emission from ^{24}Na in the NaOH grains mimics the ^{40}K beta emission from feldspar grains in sandy sediment. Provided the overall mass is small, the probability of gamma interaction is low. The dose deposited within individual quartz grains in the experimental set-up was determined using single-grain OSL measurements.

2.2 Equipment and protocols

The sand-box mixture contained two principal materials, quartz (5.06 g) and NaOH (0.39 g, giving 8% by volume). A small quantity (0.07 g) of Al_2O_3:C grains was also included, but not used in the analysis. The quartz grains were taken from a sand dune on the coast of the Netherlands. Grains of 180–212 μm diameter were isolated by sieving, and chemically treated with HCl, H_2O_2 and HF. The quartz was bleached for several hours in a solar simulator; the residual OSL signal from the quartz was equivalent to 0.016 ± 0.004 Gy. NaOH grains (mesh 20-40, 97% purity) were purchased from Perkin Elmer and sieved in a nitrogen atmosphere to obtain the grain size fraction 600–850 μm. The NaOH was pre-screened to ensure that radioactive impurities would not be induced by neutron activation.

The pseudo-feldspar (NaOH) grains in this experiment are far larger than the quartz grains, resulting in a sediment mixture that is unlikely to occur in nature. This mixture was designed so that the spread in observed D_e caused by beta-dose heterogeneity would make other sources of scatter insignificant.

Irradiation Procedure

A polyethylene sample tube containing the NaOH grains was irradiated for 85 s at a neutron flux of 4.59×10^{12} n cm^{-2} s^{-1}. The activated NaOH was given a cooling period of 26 hours, to allow the short-lived activation products to decay. Following this, the sample tube was placed into a lead container, and the quartz grains then added to the NaOH. The sealed container was vigorously shaken by hand, and placed in storage. After two weeks (22 half-lives of ^{24}Na), the mixture was opened in a dark-lab, and the (water-soluble) NaOH washed out. A scale drawing of the experimental apparatus is shown in Fig. 2.

OSL measurements

Single-grain OSL measurements were performed using a Risø TL/OSL-DA-15 reader with single-grain attachment (Bøtter-Jensen et al., 2000). Individual grains were stimulated with an Nd:YVO_4 diode-pumped laser (λ = 532 nm), delivering ~50 W cm^{-2}. The detection filter was a 2.5 mm Hoya U340, shown by Ballarini et al. (2005) to optimize signal collection. OSL measurements followed a single-aliquot regenerative-dose protocol (Murray and Wintle, 2000), modified for single-grains from young samples following Ballarini et al. (2007), and equivalent to the multi-grain protocol used to date the same quartz (Cunningham et al., 2011). The details are given in Table 1. OSL signals were measured for 0.83 s each, recorded in 50 time-bins of 0.017 s. We used the early background approach for signal analysis (Cunningham and Wallinga, 2010), with the first 0.23 s used for the initial signal, and the subsequent 0.60 s used for background. To reduce measurement time, we checked the sensitivity of each grain after the first test dose (formula of Li (2007)), continuing to measure only those grains with relative standard error on the test-dose OSL of less than 6.5 % (an arbitrary threshold). The dose-response curve was constructed with a saturating exponential function. Uncertainties on D_e were calculated with a Monte Carlo process, plus an additional term accounting for the appropriateness of the saturating exponential fit (Duller, 2007). We measured the response of each sensitive grain to a zero dose (recuperation test) and repeated dose (recycling ratio test); grains were accepted if recuperation was less than 0.2 Gy, and the recycling ratio was between 0.90 and 1.10. Irradiation was administered with the inbuilt $^{90}Sr/^{90}Y$ beta source, providing ~0.12 Gy s^{-1} to grains in the sample position. The dose rate to each single-grain position was calibrated separately.

2.3 Experimental results

The D_e was determined for 89 individual grains of quartz, which had been irradiated in the sand-box described above. There is a large amount of scatter in D_e, which ranges from 0.26 Gy to 19.2 Gy (Fig. 3a); using the central age model (Galbraith et al., 1999), the dose obtained is 2.52 ± 0.24 Gy, with overdispersion of 0.82 ± 0.07 (see section 4.1 for explanation of these terms). Part of the scatter is likely to be due to non-perfect measurement reproducibility using the single-grain reader. Previous experiments have shown that an apparently uniform gamma dose given to quartz grains induces more scatter in the OSL data than can be explained by counting statistics alone (Kalchgruber et al., 2003; Thomsen et al., 2005; 2007). The cause of this scatter is not certain, but it does need to be accounted for when estimating scatter from other sources. We therefore

carried out single-grain OSL measurements on the bleached quartz, after irradiating a batch with gamma rays from a ^{60}Co source. The apparatus used for the irradiation is crucial in providing a uniform gamma-dose; we used the apparatus described in Bos et al. (2006), minus the Fricke solution. The precise dose administered is not known (the calculation is complicated by the time taken to load the sample into position). Twenty-six grains were accepted, giving a 'central' dose of 4.65 ± 0.17 Gy, and overdispersion of 0.17 ± 0.03 (Fig. 3b). This overdispersion (17%) in the gamma-dose recovery incorporates all possible sources of scatter besides the heterogeneous beta dose. The much larger overdispersion found in the sand-box data (82%) is therefore almost entirely due to beta-dose heterogeneity.

3. Monte Carlo Simulations

To complement the experimental work, a simulation of the experiment was performed using the Monte Carlo radiation transport code MCNP4C (Briesmeister, 2000). This code has previously been applied to problems of dose determination in sediment (Nathan et al., 2003; Cunningham et al., 2011).

3.1 Geometry

Monte Carlo simulations were designed to replicate the experimental simulations as closely as possible. A cross section of the simulation geometry can be seen in Fig. 2. The plastic and lead containers were cylindrical. The placement of the grains was carried out as follows:

1. Source grains were randomly selected from the measured distribution of NaOH grain size. This distribution was carefully measured by taking photographs of NaOH grains with a digital camera attached to a microscope, and comparing their diameters to a ruler photographed at the same scale. Random selection continued until the combined mass of the grains reached 0.39 g.
2. The source grains were randomly placed inside the polyethylene sample tube, with the condition that no grains overlapped. The height of the permissible region was determined by the mass of the combined quartz and NaOH, assuming a packing density of 53%. This packing density was found to be appropriate to the experimental simulation, after weighing the same quartz in a container with known volume. Ninety-nine spherical quartz dosimeter grains of 196 μm diameter were added, using the same placement conditions.

The total sediment volume was reduced to 95% of the true experimental volume, to ensure computational limits were not exceeded. The modelled sediment contained ~950 NaOH source grains and 99 quartz dosimeters. The remaining volume (89.5% of the sediment volume) was defined as quartz, with density of 1.41 g cm^{-3}, i.e. the average density when pore space is included. This represents a significant simplifying assumption. The alternative would be to assume all grains are spherical, and use an algorithm to pack the spheres into the correct density. However, this approach would present complications: the packing of spheres to a realistic density is not a trivial problem, and there are computational limits on the number of cells and the number of sources that can be modelled. These limits would be far exceeded if every grain were to be included individually.

3.2 Sources and tallies

Each geometry was used in two separate runs, one with beta particles, one with γ-ray photons. The beta spectrum (Fig. 1) and discrete γ-ray energies of ^{24}Na were obtained from the ENSDF database via ie.lbl.gov in March 2011. For the beta model, 10 million histories were run. The beta spectrum was artificially biased towards the high end. That is, the probability of emission in the high-end tail of the beta spectrum was artificially increased, while at the same time the weight of the emitted beta particles was decreased by the same factor to obtain unbiased results. Such source biasing improves the sampling of the high-end tail of the beta spectrum. This reduces the computation time required for precise results.

Twenty million histories were initiated in the gamma model. We set the importance of the lead container to 5%: this function terminates the majority of particles which enter the lead container, and increases the weight of the remainder by a corresponding amount. This is necessary because the gamma photons are more likely to interact with the larger mass of the lead than with the quartz, but the interaction with the lead is not of interest besides the small percentage of Compton-scattered photons re-entering the quartz, and Pb X-rays.

All simulations were performed in coupled photon-electron mode, using the el03 and mcnplib2 electron and photon interaction data libraries and selecting the ITS electron energy indexing algorithm (Schaart et al., 2002). The upper photon and electron energy limits were set to 4.3 MeV. The photon and electron cut-off energies were set to 1 keV and 10 keV, respectively. Other simulation parameters were left at the default setting.

The energy deposited in each of the 99 dosimeter grains was recorded using the *F8 tally. The mean uncertainty on the dosimeter tallies for the combined beta and gamma models was 5%, smaller than most of the experimental uncertainties.

3.3 Model results

An analysis of the Monte Carlo results is presented in Figs 4 and 5. In Fig. 4, the energy recorded in each dosimeter grain is plotted as a function of grain location. Considering the beta-derived energy only, it can be seen that the majority of the scatter between grains is unrelated to radial distance (Fig. 4a) or height (Fig. 4c). However, on the edge of the sand volume (radial distance > 0.65 cm) there is a cluster of low points. The low points are caused by disequilibrium in the flux of charged particles, as those particles escaping the sediment volume are not compensated by any incoming particles. The same effect can be seen for grains located close to the base or top of the sand volume (Fig. 4c). A similar issue also influences the energy recorded under the gamma-only conditions, although a much greater number of dosimeters are affected. The energy deposited in each dosimeter grain is negatively correlated with the distance to the nearest source grain (Supplementary Fig. 1).

Fig. 5 shows the output of the Monte Carlo simulations plotted as a series of histograms. The combined results of the beta and gamma runs can be seen in Fig. 5c; these data are used for comparison with the experimental results. Figure 5d plots the same data, but excluding grains that are located close to the edge of the sand volume. This provides an indication of the distribution that could be expected under charged-particle equilibrium (although the wall effects still apply to the gamma component).

4. Comparison of experiment and Monte Carlo simulations

4.1 Statistical description of data

For comparison of the experimental and modelled distributions, it is useful to identify a statistic which describes the scatter in the data, and which can be applied to all datasets. This could be done by fitting a suitable model to the data. The positively skewed distributions of the modelled and measured data lend themselves to fitting with a log-normal function. However, such a procedure should not be performed on the histograms directly, because each datapoint comes with an error term that must also be considered. The best approach is to use a maximum likelihood estimator (MLE) to identify the most

likely parameters of the log-normal function. In fact, just such a procedure is used frequently in the OSL dating literature, and is known as the Central Age Model (CAM) of Galbraith et al. (1999). The application of the CAM to a dataset of D_e (with error terms) determines the 'central age' and 'overdispersion (σ)', which together describe the form of the underlying log-normal distribution. For our purposes, the central age is not relevant, but σ may give a good indication of the relative spread in the data.

The suitability of a log-normal function for analysing the data can be visualised with quantile plots (Fig. 6). Quantile plots graph the sorted data against the theoretical quantiles of the chosen distribution; if the sample was drawn from the specified distribution, the datapoints would appear in straight line. Thus the experimental data (Fig. 6a) and model data (Fig 6b) are reasonably described by a log-normal distribution. Both plots show a slight departure from linearity at the negative end: the log-normal distribution is not a perfect fit. In the low-dose region, the experimental data (Fig. 6a) have higher doses, and the model data (Fig. 6b) have lower doses than would be expected from a log-normal distribution. The use of standardised residuals for the x-axis is to account for the non-uniform uncertainties on the data (Galbraith and Roberts, 2012).

Figure 6c plots the experimental quantiles against the model quantiles; a straight line in this plot would indicate that the model data is distributed in the same way as the experimental data, without reference to any particular distribution. The concordance between the two distributions is respectable, except for the low-dose region where the contrast in the two datasets is clearer.

The sand-box experiment yielded σ of 0.82. The σ inherent in the measurement process can be estimated from the gamma-dose-recovery test, which yielded σ of 0.17. By subtracting the latter from the former, in quadrature, we can estimate the overdispersion caused by the heterogeneous distribution of beta sources as 0.80. In contrast, the Monte Carlo model yields σ of 0.50. The model underestimates the degree of scatter in the experimental results, although the shape of the distribution is correctly predicted. In an attempt to understand the source of the discrepancy, a series of sensitivity tests of the model were conducted by varying various model parameters; these tests are detailed in the following section.

4.2 Model sensitivity

Random uncertainty in the placement of the source grains

The random placement of source and dosimeter grains within the model geometry could lead to random variation in the model (or experimental) output. This effect would be

more severe for smaller numbers of source and dosimeter grains. Two sensitivity tests were conducted to determine the extent of this effect. Firstly, the model was run five times with source grains in the same position, but with the 99 dosimeter grains placed in new random positions each time. There was no significant difference in the results (mean σ of 0.48, standard deviation 0.03), indicating that the number of dosimeter grains is sufficient. Secondly, the central model was run 5 times using new random placements for both the dosimeter and source grains. These gave a mean σ of 0.49 with standard deviation 0.05, showing that the model outcome is not sensitive to the randomness in grain placement.

Mixing of materials

The model assumes that the source grains in the experiment are placed with equal probability throughout the sediment mixture. This assumption may not hold for the experiment due to the different grain sizes involved and the hand mixing of materials. The model's sensitivity to the quality of the mixing was tested by adding a rejection step to the placement of source grains, such that the probability of rejection was dependent on the y-position of the source grain. As the source grains are positioned before the dosimeter grains, the position of dosimeter grains is automatically biased in the opposite direction. The outcome of these model variations is shown in Fig. 7a, with the probability gradients visualised in the inset. Overdispersion is shown to be insensitive to a small inconsistency in the mixing. The measured overdispersion can only be replicated with a very poorly mixed sample, where the source grains are three times more likely to be located in one half of the container than the other.

Source dimensions

Great care was taken to measure the precise size of the NaOH grains (section 3.1). However, a systematic error in the microscopic measurement of NaOH grain diameter would imply a much larger error in NaOH grain volumes; an influence on measured overdispersion would then be expected. Figure 7b shows the sensitivity of the model to a systematic error in NaOH grain size. The combined source mass is unchanged, thus larger source-grain sizes equate to fewer source grains. It is clear from Fig. 7b that a feasible error in measurement of grain diameter would not account for the discrepancy between the measured and modelled overdispersion.

Total source mass

The total mass of NaOH used in the experiment was 0.39 g, measured on laboratory scales. An error in this measurement might induce a discrepancy in the results. However, it is clear from Fig. 7c that a very large error in the measurement of total source mass would be needed to account for the difference.

5. Discussion

Understanding the natural range of dose rates delivered to quartz grains in sediment would help provide more accurate and precise OSL dating. For predicting the equivalent-dose distribution arising through beta-dose heterogeneity, Monte Carlo radiation transport codes are obvious tools to use. Several different codes are available and used in applications across radiation sciences, with proven success.

The model presented in this paper was formulated using MCNP4C, and is able to predict the general form of the equivalent-dose distribution in the experimental set-up. However, the model significantly underestimates the overdispersion in the measurements. Model sensitivity tests show that the difference is greater than can be explained by random fluctuations in experimental conditions; only extreme bias in the location of modelled source grains can replicate the observed overdispersion. As there was no experimental check on the quality of the mixing, this effect cannot be ruled out. However, the shape of the modelled distribution under the poorly-mixed scenario is a poor match to the measured distribution (Supplementary Fig. 2), so poor-mixing by itself is not a satisfactory explanation. Future experiments should incorporate a post-irradiation check on the mixing efficacy, for instance by chemical analysis of different volume slices, or through micro-CT scans.

The source of the discrepancy could also lie in the parts of the real world that are not included in the model, such as the grain packing. The model geometry includes all source grains (~950) and 99 dosimeter quartz grains. All other quartz grains are treated as a uniform mass, with density lowered to account for pore spaces. In the experiment, beta particles traverse grains as well as pores. The percentage of the total path length spent in pores will vary per particle. Hence, the assumption of a homogenous medium in between the source and dosimeter grains in the simulation might result in underestimation of the overdispersion in the doses received by dosimeter grains.

Sophisticated grain-packing algorithms are available, and have been used by Nathan (2010) in combination with a different transport code. While it would not be possible to model every grain in this experiment, a grain-packing algorithm could be used in a small-scale test to determine the validity of the average-density assumption.

However, such a test should not be formulated with MCNP4C because of a systematic error encountered at cell boundaries (Schaart et al, 2002).

6. Conclusion

The deposition of ionising radiation in sandy sediment is not uniform across all grains; the prediction of equivalent-dose distributions that arise through beta-dose heterogeneity would increase precision and accuracy in OSL dating. This paper has introduced a new means of research to attack the topic. The key conclusions are:

- Artificially produced ^{24}Na can be used to mimic the dose delivered by ^{40}K hotspots in natural sediment.
- Simulations using a Monte Carlo radiation transport code are a feasible means of predicting dose distributions in sediment. The model formulated in this paper underestimates the degree of scatter in the experimental results. Model deficiencies may be culpable.
- The combination of Monte Carlo simulation with controlled experimental validation could provide a framework for increased understanding of dose-rate heterogeneity in sediment. Ultimately, a general model to predict dose-rate heterogeneity would prove invaluable for OSL dating; the procedure outline here could help to achieve that goal.

Acknowledgments

The authors are indebted to many people at the Reactor Institute Delft for making this project possible. In particular, Adrie Bos, Jakob Wallinga, Gert-Jan Auwerda, Marc Korevaar and Peter Bode gave advice and assistance. The radiation safety team helped perform the experiment. We thank the anonymous reviewers for their constructive comments. AC was funded through NWO/STW grant DSF.7553.

References

Arnold, L.J., Roberts, R.G. 2009. Stochastic modelling of multi-grain equivalent dose (De) distributions: Implications for OSL dating of sediment mixtures. Quaternary Geochronology 4, 204-230.

Ballarini, M., Wallinga, J., Duller, G.A.T., Brower, J.C., Bos, A.J.J., van Eijk, C.W.E. 2005. Optimizing detection filters for single grain optical dating of quartz. Radiation Measurements 40, 5-12.

Ballarini, M., Wallinga, J., Wintle, A.G., Bos, A.J.J. 2007. A modified SAR protocol for optical dating of individual grains from young quartz samples. Radiation Measurements 42, 360-369.

Bos, A.J.J., Wallinga, J., Johns, C., Abellon, R.D., Brouwer, J.C., Schaart, D.R., Murray, A.S. 2006. Accurate calibration of a laboratory beta particle dose rate for dating purposes. Radiation Measurements 41, 1020-1025.

Bøtter-Jensen, L., Bulur, E., Duller, G.A.T., Murray, A.S. 2000. Advances in luminescence instrument systems. Radiation Measurements 32, 57-73.

Briesmeister, J.F. 2000. MCNP – A General Monte Carlo N-Particle Transport Code Version 4C. Report LA-13709-M (Los Alamos National Laboratory).

Cunningham, A.C., Wallinga, J. 2010. Selection of integration time intervals for quartz OSL decay curves. Quaternary Geochronology 5, 657-666.

Cunningham, A.C., Bakker, M., van Heteren, S., van der Valk, B., van der Spek, A.J.F., Schaart, D.R., Wallinga, J. 2011. Extracting storm-surge data from coastal dunes for improved assessment of flood risk. Geology 39, 1063-1066.

Duller, G.A.T., 2007. Assessing the error on equivalent dose estimates derived from single aliquot regenerative dose measurements. Ancient TL 25, 15-24.

Duller, G.A.T., 2008. Single-grain optical dating of Quaternary sediments: why aliquot size matters in luminescence dating. Boreas 37, 589-612.

Galbraith, R.F., Roberts, R.G. Statistical aspects of equivalent dose and error calculation and display in OSL dating: an overview and some recommendations. Quaternary Geochronology, in press.

Galbraith, R.F., Roberts, R.G., Laslett, G.M., Yoshida, H., Olley, J.M. 1999. Optical dating of single and multiple grains of quartz from jinmium rock shelter, northern Australia, part 1, Experimental design and statistical models. Archaeometry 41, 339-364.

Grine, F.E., Bailey, R.M., Harvati, K., Nathan, R.P., Morris, A.G., Henderson, G.M., Ribot, I, Pike, A.W.G. 2007. Late Pleistocene human skull from Hofmeyr, South Africa, and modern human origins. Science 315, 226-229.

Kalchgruber, R., Fuchs, M., Murray, A.S., Wagner, G.A. 2003. Evaluating dose-rate distributions in natural sediments using α-Al_2O_3:C grains. Radiation Measurements 37, 293-297.

Li, B. 2007. A note on estimating the error when subtracting background counts from weak OSL signals. Ancient TL 25, 9-14.

Mayya, Y.S., Morthekai, P., Murari, M.K., Singhvi, A.K. 2006. Towards quantifying beta microdosimetric effects in single-grain quartz dose distribution. Radiation Measurements 41, 1032-1039.

Murray, A.S., Wintle, A.G. 2000. Luminescence dating of quartz using an improved single-aliquot regenerative-dose protocol. Radiation Measurements 32, 57-73.

Nathan, R.P., 2010. Numerical modelling of environmental dose rate and its application to trapped-charge dating. DPhil thesis, Oxford.

Nathan, R.P., Thomas, P.J., Jain, M., Murray, A.S., Rhodes, E.J. 2003. Environmental dose rate heterogeneity of beta radiation and its implications for luminescence dating: Monte Carlo modelling and experimental validation. Radiation Measurements 37, 305-313.

Rhodes, E.J. 2011. Optically stimulated luminescence dating of sediments over the past 200,000 years. Annual Review of Earth and Planetary Sciences 39, 461-488.

Schaart, D.R., Jansen, J.T.M., Zoetelief, J., de Leege, P.F.A. 2002. A comparison of MCNP4C electron transport with ITS 3.0 and experiment at incident energies between 100 keV and 20 MeV: influence of voxel size, substeps and energy indexing algorithm. Physics in Medicine and Biology 47, 1459-1484.

Thomsen, K.J., Murray, A.S., Bøtter-Jensen, L. 2005. Sources of variability in OSL dose measurements using single grains of quartz. Radiation Measurements 39, 47-61.

Thomsen, K.J., Murray, A.S., Bøtter-Jensen, L., Kinahan, J. 2007. Determination of burial dose in incompletely bleached fluvial samples using single grains of quartz. Radiation Measurements 42, 370-379.

Wintle, A.G. 2008. Fifty years of luminescence dating. Archaeometry 50, 276-312.

Figure and table captions

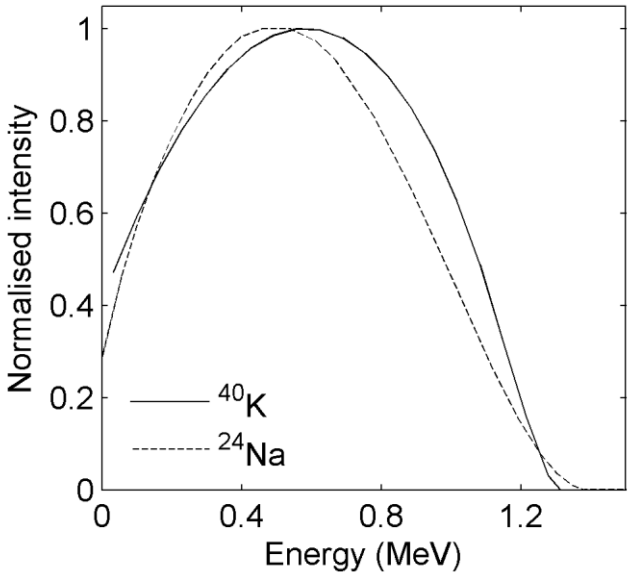

Fig. 1. Beta-energy spectra of ^{40}K and ^{24}Na. The ^{24}Na spectrum extends to 4 MeV at very low probability, and is not shown in the figure.

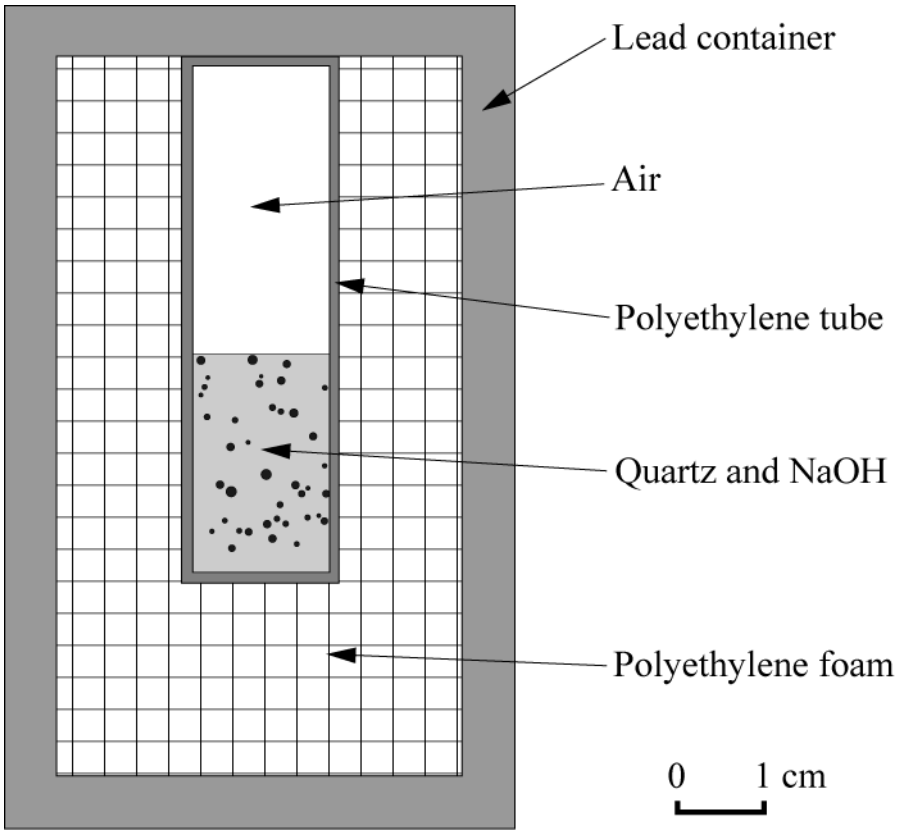

Fig. 2. Scale drawing of a cross-section of the experimental set-up; containers are cylindrical. The dark circles represent the randomly positioned NaOH spheres, obtained from a cross-section of the model geometry.

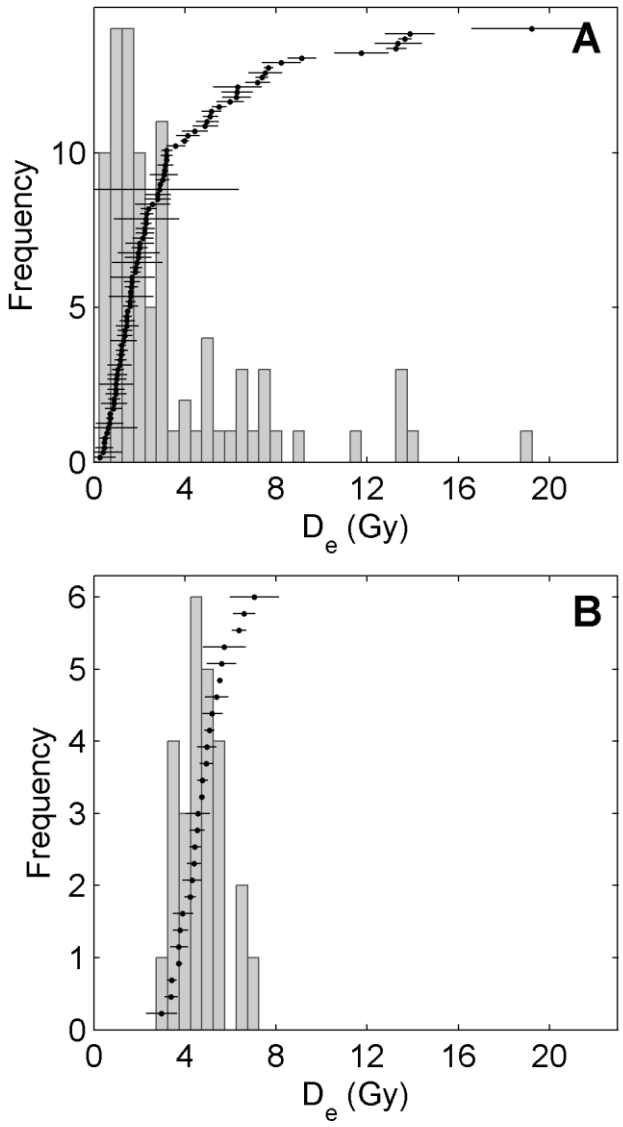

Fig 3. Experimental results. (a) Histogram showing the single-grain D_e distribution of the sand-box quartz, overlain by the empirical distribution. Overdispersion is 0.82 ± 0.07. (b) Single-grain D_e measured after administering a uniform gamma dose from an external ^{60}Co source. Overdispersion is 0.17 ± 0.03. Histogram bin width is 0.5 Gy in both plots.

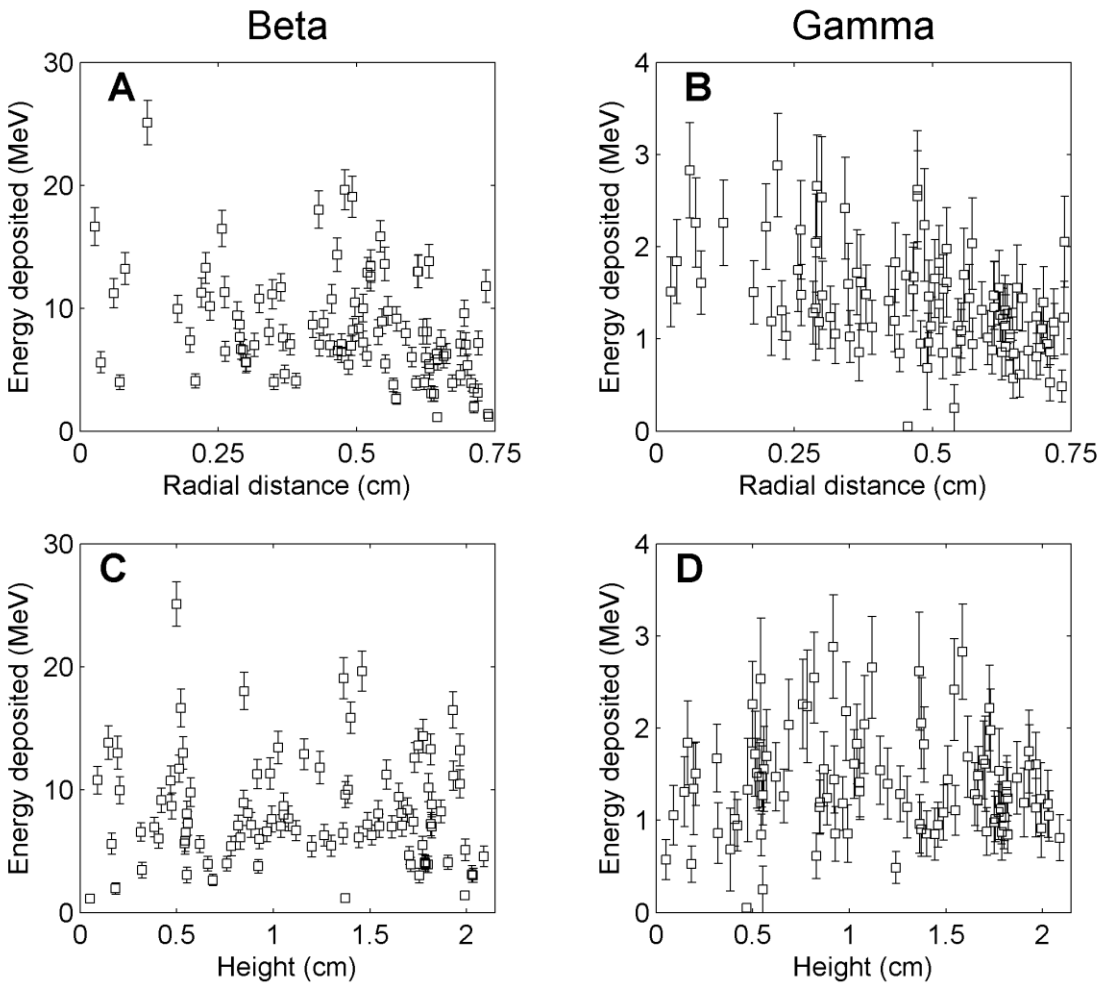

Fig. 4. Monte Carlo simulations of the energy deposited to individual grains of quartz in the experiment described in section 2, plotted as a function of grain location. On the left-hand side, the energy deposited due to the ^{24}Na beta emission from the NaOH grains: (a) according to the distance of each grain from the central axis of the cylindrical container, (c) according to the height position of each grain. On the right-hand side, (b) and (d) plot the same information for the gamma emission from ^{24}Na. In all cases, the y-axis show the energy deposited after 10 million disintegrations (with each disintegration yielding one beta electron and two gamma rays). One-sigma error bars are shown.

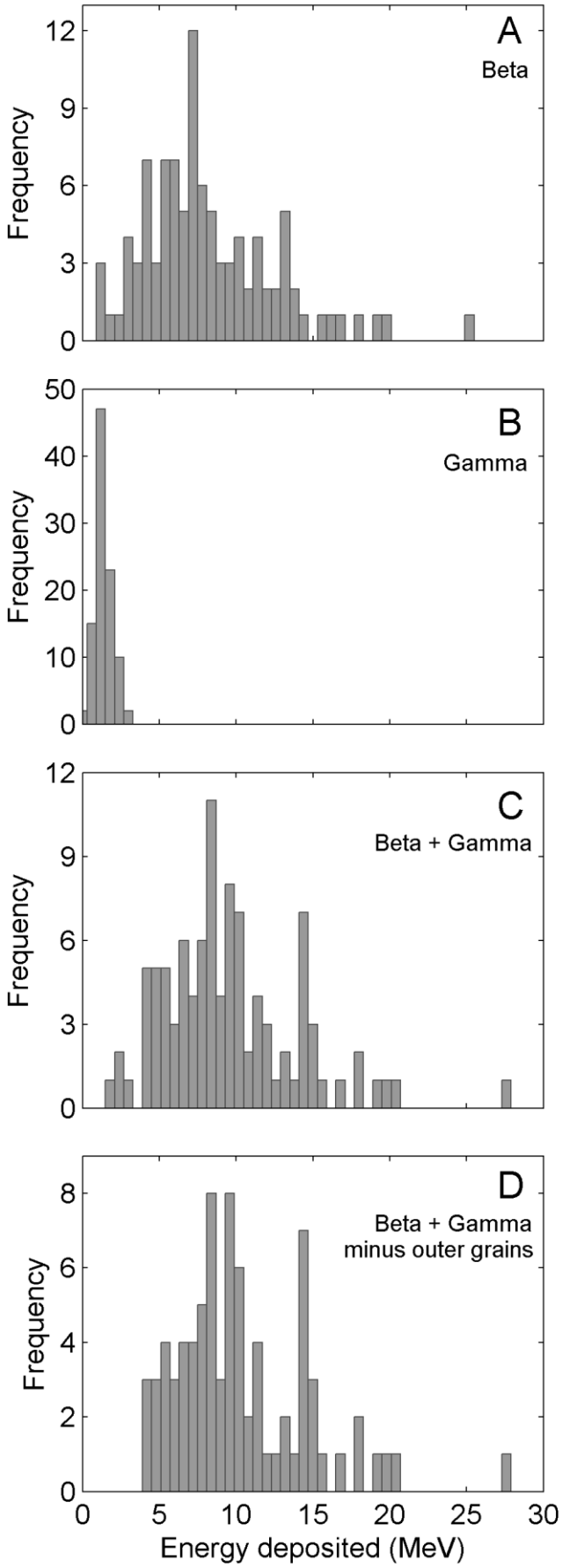
A
Beta
B
Gamma
C
Beta + Gamma
D
Beta + Gamma
minus outer grains
Frequency
Energy deposited (MeV)
0
5
10
15
20
25
30

Fig. 5. Histograms showing the output of the Monte Carlo simulations. The x-scale indicates the energy deposited in the dosimeter cells after 10 million disintegrations; bin width is 0.6 MeV in all cases. (a) Beta dose only; (b) Gamma dose only; (c) Sum of beta and gamma contributions; (d) same as (c), but only for grains lying at least 1 mm away from all edges of the sand/NaOH region. Graphs (a) to (c) contain 99 datapoints, graph (d) has 80.

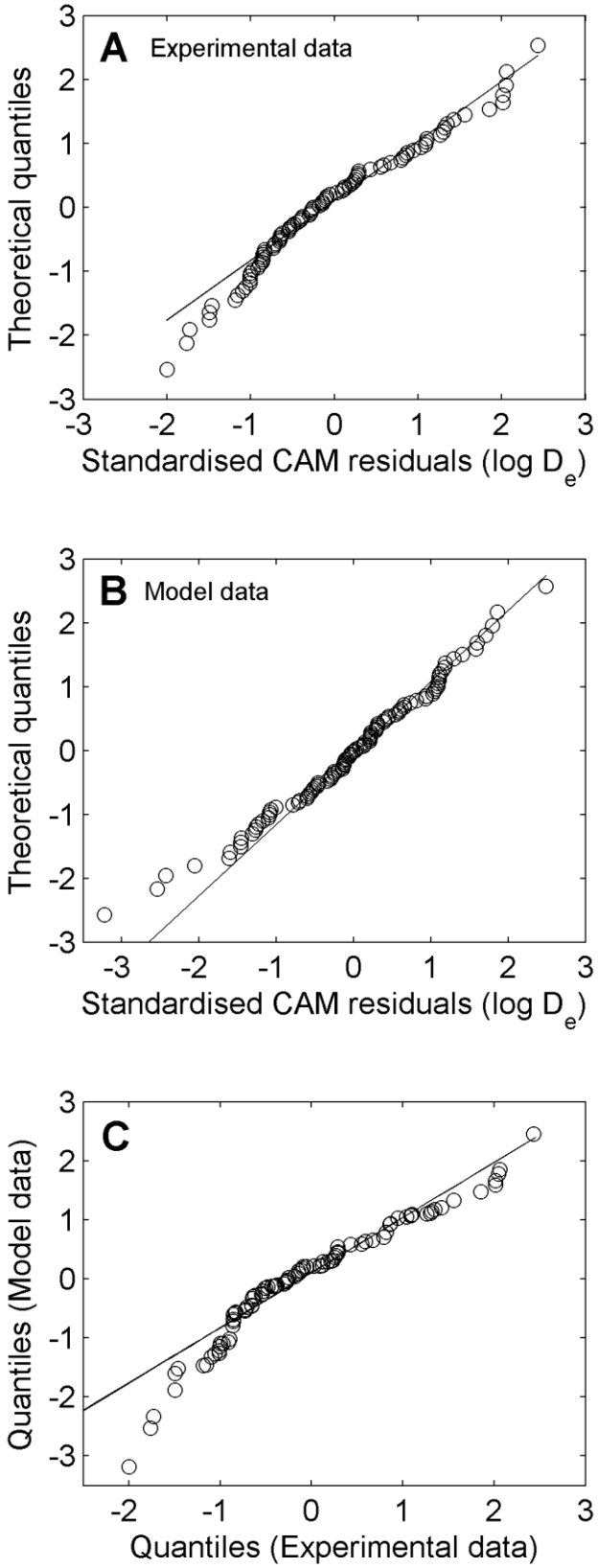
A
Experimental data
Theoretical quantiles
Standardised CAM residuals (log D_e)
B
Model data
Theoretical quantiles
Standardised CAM residuals (log D_e)
C
Quantiles (Model data)
Quantiles (Experimental data)

Fig. 6. Quantile plots of experimental and model data. (a) The standardised CAM residuals from the experimental data plotted against the theoretical quantiles. The straight line is plotted through the 0.25 and 0.75 quantiles. Approximate linearity in the data indicates that the data may be drawn from a log-normal distribution. (b) Similar plot for model data from the central run. All modelled grains are used, including those at the edges of the container. (c) The CAM-residual derived quantiles for the two datasets plotted against one another. Linearity in this plot indicates similarity in shape between the two datasets.

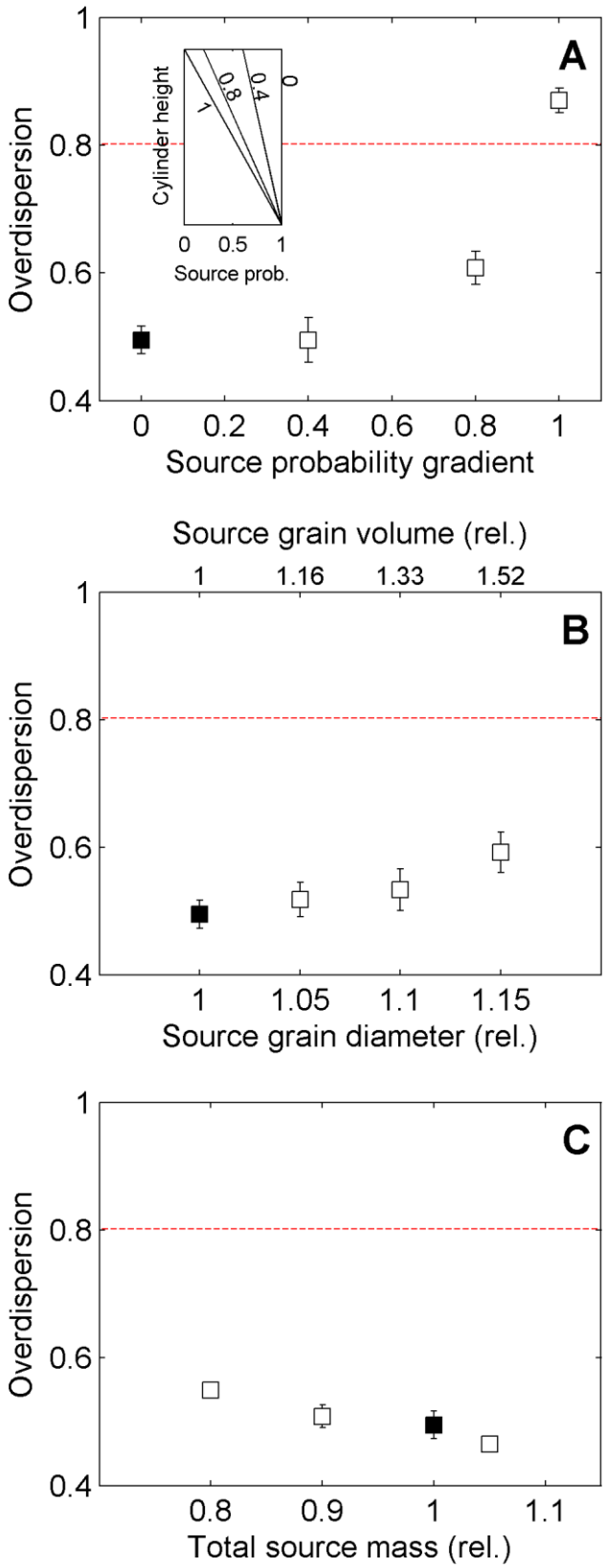
A
Overdispersion
1
0.8
0.6
0.4
0
0.2
0.4
0.6
0.8
1
Source probability gradient
Cylinder height
1
0.8
0.4
0
0
0.5
1
Source prob.
Source grain volume (rel.)
1
1.16
1.33
1.52
B
Overdispersion
1
0.8
0.6
0.4
1
1.05
1.1
1.15
Source grain diameter (rel.)
C
Overdispersion
1
0.8
0.6
0.4
0.8
0.9
1
1.1
Total source mass (rel.)

Fig. 7. Sensitivity of model overdispersion to variations in the model parameters. Each datapoint shows the arithmetic mean and standard deviation of three model runs (five for the central point, shown in black). Dashed line indicates the measured overdispersion from experimental data, after subtracting in quadrature the overdispersion measured following a uniform gamma dose. (a) Non-uniformity in the distribution of source grains. The height of the source grains in the model are selected from the probability distributions shown in the inset. The x-axis indicates the top-to-bottom probability gradient. (b) Sensitivity to the diameter of the source grains, relative to the measured grain size distribution (600-850 μm). Relative grain volumes are indicated in the upper x-axis. The total source volume is the same for all points, so an increase in grain diameter means fewer source grains (c) Sensitivity to the total source mass, relative to the measured source mass of 0.39 g. The grain sizes are the same for all points, so a decreased total source mass means fewer grains.

Treatment	Conditions
Dose	Nat, 2.4,6,12,18,0,2.4 Gy
Preheat	180ºC, 10 s
SG OSL	125ºC, 1 s
OSL bleach	125ºC, 40 s, Blue diodes
(Test) Dose	3 Gy
Preheat	170ºC, 0 s
SG OSL	125ºC, 1 s
OSL bleach	125ºC, 40 s, Blue diodes
OSL bleach	180ºC, 40 s, Blue diodes

Table 1. Measurement protocol used for determination of $D_{e,}$ for single grains of quartz.

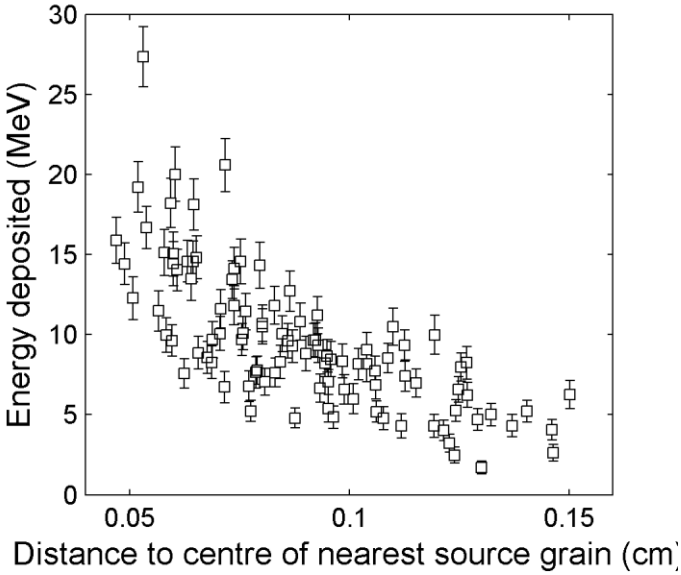

Supplementary Fig. 1. For modelled data, the energy deposited in each dosimeter grain is plotted as a function of the distance between each dosimeter and its nearest source grain (grain centre to grain centre). The inverse square law means that the nearest source grain is responsible for much energy received by a grain.

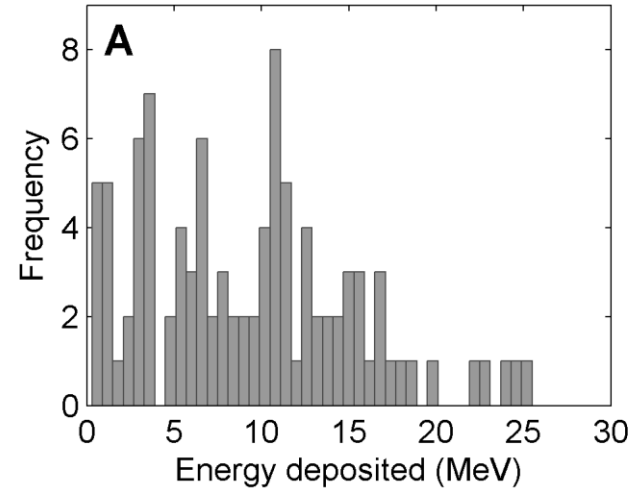
A
Frequency
Energy deposited (MeV)
0
2
4
6
8
0
5
10
15
20
25
30

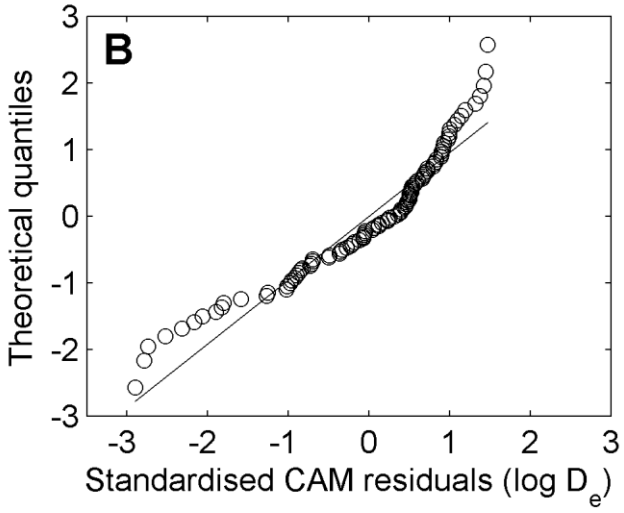
B
Theoretical quantiles
Standardised CAM residuals (log D_e)
-3
-2
-1
0
1
2
3

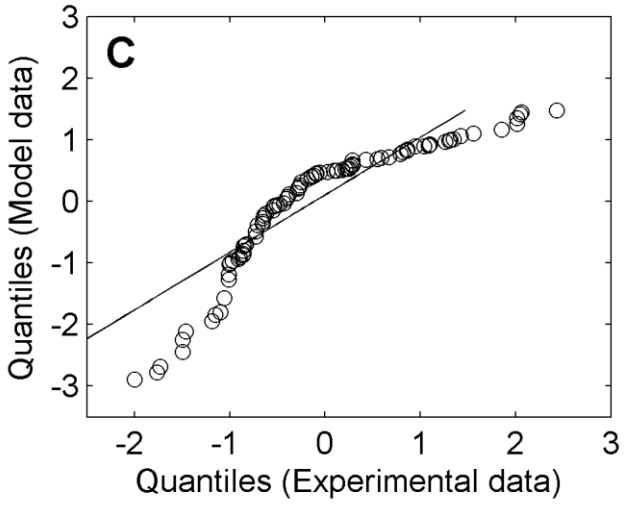
C
Quantiles (Model data)
Quantiles (Experimental data)
-3
-2
-1
0
1
2
3

Supplementary Fig. 2. Modelled data from a poor-mixing scenario (source probability gradient of 1, Fig. 7a). (a) Histogram of the energy deposited to grains in this model run. (b) The standardised CAM residuals from the model data plotted against the theoretical quantiles. The straight line is plotted through the 0.25 and 0.75 quantiles. Departure from linearity in this plot indicates that the log-normal distribution is not a good fit for the data. (c) The quantiles from the modelled data under a poor-mixing scenario are plotted against the quantiles from the experimental data. The strong non-linearity in this plot shows that the two distributions have different forms. This indicates that poor mixing in the experimental set-up is not a sufficient explanation for the discrepancy between the modelled and measured overdispersion.